Pectin degradation accounts for apple tissue fragmentation during thermomechanical-mediated puree production

Alexandra Buergy, Agnès Rolland-Sabaté, Alexandre Leca, Xavier Falourd, Loïc Foucat, Catherine M.G.C. Renard

Pectin degradation accounts for apple tissue fragmentation during thermomechanical-mediated puree production

Alexandra Buergy[a], Agnès Rolland-Sabaté[a,*], Alexandre Leca[a], Xavier Falourd[b,c], Loïc Foucat[b,c], Catherine M. G. C. Renard[d]

[a] *INRAE, Avignon Université, UMR SQPOV, F-84000, Avignon, France*

[b] *INRAE, UR BIA, F-44000, Nantes, France*

[c] *INRAE, BIBS facility, F-44000, Nantes, France*

[d] *INRAE, TRANSFORM, F-44000, Nantes, France*

[*] Corresponding author.

INRAE, UMR408 SQPOV « Sécurité et Qualité des Produits d'Origine Végétale », 228 route de l'Aérodrome, CS 40509, F-84914 Avignon cedex 9.

E-mail address: agnes.rolland-sabate@inrae.fr (A. Rolland-Sabaté).

Abstract

The relationship between fruit and puree's characteristics is still poorly understood. In particular, it is not understood how pectin solubilisation and degradation alter the texture of plant-cell dispersions and how a targeted application of processing conditions can be used to design naturally textured food products. Systematic combinations of thermal and mechanical treatments with three different temperatures (70, 83, 95 °C) and grinding speeds (300, 1000, 3000 rpm), applied on one-month (T1) and six-months stored (T6) apples, were used to generate apple purees with contrasted structural and textural characteristics. For T1, serum viscosity increased with increasing temperature (8 to 104 mPa.s) with a marked increase in pectin solubilisation (1 to 6 mg/g serum). Pectin macromolecular size and

(arabinose+galactose)/rhamnose ratio, estimating pectin side chain branching, decreased with temperature. For T6, pectin showed decreased galactose, leading to facilitated cell separation, low serum viscosity (~16 mPa.s) and restricted impact of process conditions on pectin composition and structure. Grinding had limited impact on pectin solubilisation for T1 and T6 but strongly impacted particle size (498–1096 µm for T1 or 320–1068 µm for T6) and puree's viscosity (871–1475 mPa.s for T1 or 853–1453 mPa.s for T6). Tissue fragmentation was favoured by temperature increase for T1 and by the maturation of raw apples. Process parameters induced differences in the puree's structure and texture depending on the maturation level of raw apples. The observed changes were linked to pectin degradation and substantial side chain loss.

Malus x *domestica* Borkh.; Texture; Rheology; Particle size; Cell separation; Polysaccharide

1. Introduction

Plant-based purees are suspensions of individual cells and cell clusters (pulp) dispersed in an aqueous phase (serum) (Rao, 1992). The texture is an important quality characteristic of plant-based dispersions (Szczesniak & Kahn, 1971) driven by particle size distribution, pulp content and serum viscosity (Espinosa et al., 2011; Leverrier, Almeida, Espinosa-Munoz, & Cuvelier, 2016; Rao, 1992). These factors can be modulated by applying particular thermal and mechanical treatments on raw material in order to optimise pureed food's textural characteristics without the addition of texture-controlling agents such as starches, gums, and stabilisers. Many studies focused either on the effect of thermal (Anthon, Diaz, & Barrett, 2008; Christiaens et al., 2012) or mechanical (Espinosa et al., 2011; Moelants et al., 2012; Moelants et al., 2014) treatments. However, both heating and grinding are complementary during processing since both treatments alter the puree's structure.

53 The structural characteristics are linked to modifications in pectin structure and composition
54 (Sila et al., 2009). Pectins contribute to intercellular adhesion and cell wall porosity and
55 strength (Carpita & Gibeaut, 1993; Jarvis, 1984). However, these plant cell wall
56 polysaccharides are especially vulnerable to enzymatic and chemical degradation. Indeed,
57 pectin solubilisation during processing induces tissue softening during processing (Van
58 Buren, 1979), thus facilitating subsequent tissue disruption via mechanical treatments.
59 Pectins are complex groups of polysaccharides, comprising homogalacturonan (HG),
60 rhamnogalacturonan I (RG I) and II (RG II). HG is composed of a linear chain of α-1,4-linked
61 galacturonic acids, which can be methyl-esterified at the C6 position. The degree of
62 methylation (DM) and the distribution of ester groups over the HG backbone are crucial since
63 sequences of several consecutive non-esterified galacturonic acids can induce cross-links with
64 calcium ions (Kohn & Luknár, 1977). This mechanism may contribute to cell-cell adhesion in
65 the middle lamella. Endogenous pectin methylesterase (PME) can demethoxylate the HG
66 backbone, which can be cross-linked by calcium ions and cause an increase in cell adhesion
67 and texture (Waldron, Smith, Parr, Ng, & Parker, 1997) or be further degraded by
68 polygalacturonase (PG) (Sila et al., 2009), resulting in texture loss. While enzyme activity is
69 rapidly inactivated by heat, chemical reactions are generally promoted. Pectins are susceptible
70 to acid hydrolysis due to the acidic pH of apples (around 3.7) and other fruits. On the other
71 hand, β-elimination is less critical during fruit-based food production (Waldron, Parker, &
72 Smith, 2003).
73 Although the most studied changes are reported for HG pectins, RG I domains are also
74 sensitive to heat treatment. RG I consists of a backbone with alternating rhamnose and
75 galacturonic acid residues. Rhamnose residues can be decorated by neutral sugar side chains
76 composed of galactose and/or arabinose (Ridley, O'Neill, & Mohnen, 2001). Arabinans are
77 particularly susceptible to acid hydrolysis, followed by galactans (Green, 1967; Thibault,
78 Renard, Axelos, Roger, & Crepeau, 1993). Interestingly, "debranching" (i.e., loss of arabinans

and galactans) was associated with attenuated cell adhesion in apple fruits (Nara, Kato, & Motomura, 2001; Pena & Carpita, 2004). Additionally, RG II, which accounts for less than 10% of the pectin content, has a galacturonic acid backbone with several complex oligosaccharide side chains attached to it (Mohnen, 2008; Ndeh et al., 2017).

Only a few studies have systematically analysed the combined effect of thermal and mechanical processes on puree's texture (Day, Xu, Oiseth, Lundin, & Hemar, 2010; Lopez-Sanchez et al., 2011). Furthermore, no extensive studies have investigated the consequences of pectin degradation (thermal degradation) on mechanical processing. However, modifications in pectin composition and structure are crucial in understanding the impact of processing on plant-based food structure and texture. Herein, we evaluated particle size, pulp wet mass and serum viscosity following the application of different temperature and grinding regimes and elucidated the process-structure-function relationship of pectins and their influence on apple puree texture. As pectin modifications in the raw material linked to post-harvest storage alter puree's texture (Buergy, Rolland-Sabaté, Leca, & Renard, 2020), the impact of processing conditions was compared between apples stored for one and six months.

2. Material and Methods

2.1. Plant material

Apple (*Malus* x *domestica* Borkh.) cultivar Golden Delicious was grown in Mallemort, France and harvested in September 2018 and 2019, corresponding to the commercial harvest dates. In 2018, apples were chemically thinned using 3 L/ha PRM 12® RP (ethephon, 17 April 2018), 2 L/ha PRM 12® RP (24 April 2018), 3.5 L/ha MaxCel® (6-Benzylaminopurine) and 1.5 kg/ha Rhodofix® (1-naphthalenacetic acid, 30 April 2018) and 3.5 L/ha MaxCel® (4 May 2018). In 2019, apples were thinned with 18 L/ha ATS

105 (ammonium thiosulphate, 20 April 2019), 0.15 kg/hL Rhodofix® (27 April 2019) and 5 L/ha
106 MaxCel® (4 May 2019).
107 Apples harvested in 2018 and 2019 were stored for six months (T6) and one month (T1),
108 respectively, at 4 °C in a normal atmosphere. One day before processing, apples were divided
109 into two equal groups. The first batch was used to isolate the alcohol-insoluble solids (AIS)
110 (see section 2.4.1), the second batch was processed into a puree.
111
112 *2.2. Puree preparation*
113
114 Approximately 3 kg of apples were cored, cut into 12 pieces and processed under vacuum
115 using a cooker-cutter (RoboQbo Qb8-3, RoboQbo, Bentivoglio, Italy), equipped with two
116 micro-serrated cutting blades and a mixing blade. T1 and T6 apples were processed under
117 identical conditions (Supplementary Fig. S1). Each temperature (70, 83, 95 °C) was combined
118 with a blade rotation speed (300, 1000, 3000 rpm), resulting in nine different treatments. Each
119 process was conducted in triplicate, and each repetition was spaced by one week due to the
120 time needed for sample characterisation.
121 Since the temperature increase was longer for higher temperatures (difference of 140 s
122 between 70 and 95 °C), a low blade rotation speed of 100 rpm was applied during this period.
123 This step was employed to mix the apples without grinding them. Upon reaching the working
124 temperature, we increased the blade rotation speed and maintained this speed for 30 min. The
125 heating effects caused by blending were counteracted by the cooling system of the cooker-
126 cutter, guaranteeing a constant value (± 1 °C) around the indicated process temperature.
127 Purees were not refined, and physicochemical characterisations were carried out directly after
128 processing once the purees reached room temperature. Analytical measurements were
129 conducted on thawed samples previously stored at -20 °C.
130

2.3. Physico-chemical characterisation

2.3.1. Rheology of the purees and sera

Rheological analyses of both purees and sera were conducted at 22.5 °C as reported previously (Buergy et al., 2020), a stress-controlled rheometer (Physica MCR301) equipped with a Peltier cell (CPTD-200) and a measuring cylinder (CC27/S) from Anton Paar (Graz, Austria). For purees, the flow curve and amplitude sweep were measured using a vane measuring system (FL100/6W). Rheological analyses were not theoretically adapted for purees containing particles larger than 1 mm, since the measuring system gap was 3.46 mm. Thus, rheological values obtained for purees prepared at 70 and 83 °C and 300 rpm should be treated cautiously.

Serum viscosity was measured with a flow curve using a double gap cylinder geometry set (DG27).

2.3.2. Particle size distribution

Laser granulometry (Mastersizer 2000, Malvern Instruments, Malvern, UK) was employed to measure the particle size distribution in the puree as described by Buergy et al. (2020). The Malvern's software was used to calculate the averaged size distribution over three repeated measurements on the same sample. Each puree was analysed twice.

2.3.3. Pulp wet mass (PWM) and water retention capacity (WRC)

Each puree (3 repetitions × 9 processes) was centrifuged (7690 × g, 15 min at 15 °C) and separated into pulp and serum. The ratio of the pulp weight to the initial weight of the puree was defined as the PWM and expressed in g/100 g (Espinosa et al., 2011). The WRC of the pulp was defined as the amount of water retained by the pulp's cell wall polysaccharides and expressed in g/g dry weight (Robertson et al., 2000). The ratio of the PWM to the pulp's dry

157 weight was estimated after AIS isolation. The WRC was only analysed for samples processed
158 at 3000 rpm since these purees represented individual cells. One sample at each temperature
159 was measured, both for T1 and T6.
160
161 *2.4. Analytical*
162
163 *2.4.1. Cell wall isolation and serum precipitation*
164 Cell wall polysaccharides were extracted as AIS, using the protocol established by Le
165 Bourvellec et al. (2011). This method involves adding 700 mL of ethanol per litre of raw
166 apples to extract the AIS. Three replicates using 10 representative apples were performed, and
167 AIS yields were expressed in mg/g fresh weight (FW).
168 The pulp was washed with water and the AIS were isolated as previously described by Buergy
169 et al. (2020). The pulp's AIS yield was calculated by dividing the dry pulp weight by the
170 initial pulp weight after water-washing and expressed as mg/g FW.
171 The serum AIS were isolated by alcohol precipitation according to the method of Buergy et
172 al. (2020). The dry sample weight and the initial serum weight ratio provides a rough estimate
173 of the soluble pectin content in the continuous phase. Serum AIS yields are expressed in mg/g
174 serum FW. Since the present study focused on apples stored for one month, the AIS extraction
175 was conducted with all three T1 replicates, but only one T6 sample.
176
177 *2.4.2. Cell wall polysaccharide analysis*
178 After the acid hydrolysis of neutral sugars and the internal standard myo-inositol (Saeman,
179 Moore, Mitchell, & Millett, 1954), the free sugars were derivatised to volatile alditol acetates
180 (Englyst, Wiggins, & Cummings, 1982). Then the samples were applied to a Clarus 500 gas
181 chromatograph (PerkinElmer, Waltham, USA) equipped with a flame ionisation detector
182 (FID) and an OPTIMA® capillary column (30 m × 0.25 mm i.d., 0.25 µm film thickness,

Macherey-Nagel, Düren, Germany), and analysed at 230 °C. Helium was used as the carrier gas.

Galacturonic acid (GalA) content in the acid hydrolysate was determined spectrophotometrically using the *m*-hydroxydiphenyl assay (Blumenkrantz & Asboe-Hansen, 1973).

Methanol was quantified using the stable isotope dilution assay after saponification (Renard & Ginies, 2009). Samples were analysed on a Trace 1300 gas chromatograph (Thermo Scientific, Waltham, USA), equipped with a TG-WaxMS capillary column (30 m × 0.25 mm i.d., 0.5 µm film thickness, Thermo Scientific, Waltham, USA) and coupled to a ISQ LT single quadrupole mass spectrometer (Thermo Scientific, Waltham, USA).

The molar ratio of methanol to GalA gave the degree of methylation (DM) is expressed as a percentage (%).

2.4.3. Starch determination

We used the total starch assay kit K-TSTA (Megazyme, Wicklow, Ireland) to quantify the starch content in the AIS of serum and raw apples. The specified enzyme concentrations were doubled since residual polyphenols in the AIS might reduce enzyme activity. Each sample was analysed in duplicate. All values for AIS, neutral sugars, GalA and methanol were adjusted according to the respective starch content.

2.4.4. High-performance size-exclusion chromatography coupled to multi-angle laser light scattering (HPSEC-MALLS) and online viscometry

As described by Buergy et al. (2020), the molar mass and size distribution of soluble pectins were determined on a high-performance size-exclusion chromatography (HPSEC) system coupled to a multi-angle laser light scattering detector (DAWN HELEOS 8+ (Wyatt Technology, Santa Barbara, USA) fitted with a K5 flow cell and a GaAs laser, $\lambda = 660$ nm), a

differential refractive index detector (Shimadzu, Tokyo, Japan), an online viscometer (Viscostar III, Wyatt Technology) and a prominence diode array detector (DAD). Initial concentrations of 2.5 mg AIS/mL (serum) or 10 mg AIS/mL (raw apples) were used to extract soluble pectins directly into the eluent (acetate buffer, 0.2 M, pH 3.6). Samples were eluted at a flow rate of 0.6 mL/min at 40 °C and separated by three PolySep-GFC columns (P3000, P5000 and P6000, 300 × 7.8 mm) and a guard column, all from Phenomenex (Le Pecq, France). The ASTRA® software (Wyatt Technology, version 7.3.2.19 for PC) was used for data treatment as described by Buergy et al. (2020). The weight-average molar mass $\overline{M}_w$, the z-average intrinsic viscosity $\overline{[\eta]}_z$ and the z-average viscometric hydrodynamic radius $\overline{R}_{hz}(v)$ were obtained at the summit of the main peak. Each sample was injected once. For T1, samples of the first repetition were not considered since molar mass distribution was significantly different from the other repetitions. This discrepancy was likely due to incomplete starch degradation in these samples.

2.4.5. Nuclear magnetic resonance spectroscopy (NMR)

^{1}H-NMR was employed to visualise β-elimination products in the serum AIS and was performed according to Tjan, Voragen, and Pilnik (1974). At 4 °C, AIS (5 mg/mL) were solubilised for 1 h in distilled water before adjusting the pH to 6 with NaOH. The samples were centrifuged (4272 × g, 15 min at 4 °C) to remove possible cell wall remnants. The supernatant was freeze-dried before the sample was suspended in D_2O (0.75 mL) over night at 4 °C. The following day, the sample was freeze-dried and suspended in D_2O as before. The samples obtained were analysed at all of the temperatures (3000 rpm, T1). As a positive control, serum AIS, obtained at 95 °C, 3000 rpm and diluted to 5 mg/mL with distilled water, was heated for 30 min at 100 °C at pH 6. Afterwards, the control sample's pH was readjusted to pH 6 and treated in the same way as the samples. Samples and the control were analysed in D_2O on an NMR spectrometer (Avance III 400 NB, Bruker, Wissembourg, France) equipped

235 with a BBO 5 mm probe. We recorded 1D ^{1}H spectra at 70 °C. The most significant
236 acquisition parameters included a ^{1}H 90° pulse of 10.2 µs, 128 scans and a recycle delay of 10
237 s. Water signal presaturation was used to minimise the residual HDO signal.
238 NMR relaxation was used to monitor the interactions between the ^{1}H of water and the AIS in
239 samples ground at 3000 rpm for all temperatures. These interactions can be related to the
240 porosity of the system. For these experiments, samples from both T1 and T6 were utilised
241 since they all presented individual cells.
242 Transverse relaxation (T_2) of pulp AIS (100 mg) rehydrated in distilled water and excess
243 water gently removed, was measured at 4 °C on a Bruker Minispec mq20 (0.47 T), equipped
244 with a thermostated ^{1}H probe, using the Carr-Purcell-Meiboom-Gill pulse sequence. Echo
245 time was 1 ms, 2000 even echoes were collected, and 128 scans were acquired with a recycle
246 delay of 7 s. An inverse Laplace transformation (ILT) was applied to convert the relaxation
247 signals into a continuous distribution of the T_2 relaxation components (Lahaye, Bouin,
248 Barbacci, Le Gall, & Foucat, 2018; Saunders, Bunggyoo, Maes, Akle, & Zahr, 2012).
249
250 *2.5. Statistical analysis*
251
252 The technological repetitions were spaced by one week, and a complete protocol (temperature
253 × grinding speed) was carried out each week. Analyses were generally conducted once for
254 each of the three repetitions. Exceptions are stated in the text. The Shapiro-Wilk test was used
255 to determine if the results were normally distributed. The Kruskal-Wallis non-parametric test
256 (Kruskal & Wallis, 1952) was employed to assess differences between the samples at the 95%
257 level of significance, using the Microsoft Excel XLSTAT package (Addinsoft, 2020). Pooled
258 standard deviations (PSD) were calculated for each series of repeated measurements using the
259 sum of individual variances weighted by the individual degrees of freedom (Box, Hunter, &
260 Hunter, 1978). The R statistical software (R Core Team, 2018) was used to perform principal

component analysis (PCA) and linear regression, using the "FactoMineR" (Lê, Josse, & Husson, 2008) and "stats" packages included in the R statistical software, respectively.

3. Results and discussion

In a preliminary test (data not shown), purees were prepared at 50 and 70 °C and yielded purees with equivalent textures. It was concluded that the apple enzymes did not sufficiently degrade pectins during processing. Indeed, PG is only present in minimal amounts in apples (Wu, Szakacsdobozi, Hemmat, & Hrazdina, 1993) and is unlikely to impact apple puree's texture. Additionally, apple PME has low activity at pH 3.7 and a D-value of 0.7 min at 60°C (Z = 9.2°) (Denes, Baron, & Drilleau, 2000), which means that it is inactivated during the come-up time, and at least partially accounts for the unaltered textures of the purees in the preliminary test. Notably, 70 °C was the lowest processing temperature at which we could unequivocally evaluate the impact of the chemical reactions on apple purees. Moreover, since the heat increase speed was identical for all samples during puree processing, PME would have been able to demethylate pectins equally in all purees.

3.1. Textural characteristics of apple purees

Different process conditions led to contrasted textural characteristics of apple purees. Apparent viscosity (Fig. 1A) obtained at 70 °C and 300 rpm had a high standard deviation. This result was due to large apple cell clusters (Supplementary Fig. S2) that were not sufficiently separated by slow grinding. Consequently, the altered rheological values for the purees obtained under these conditions have limited reliability. When these results were not considered, the data show that increasing the grinding speed significantly reduced the puree's viscosity (Supplementary Table S1). While temperature did not have a significant impact,

high temperatures increased viscosity, especially at 3000 rpm. Other textural characteristics such as yield stress, G′ and G″ (Supplementary Table S1) were also significantly attenuated with increased grinding but were not influenced by temperature. The same trend was observed for T6 (Supplementary Table S1), and the effect of grinding on apparent viscosity was more pronounced since even slow grinding speeds led to homogenous puree textures (Fig. 1B). Hence, the range of apparent viscosity values was slightly reduced compared to T1. However, the storage duration did not significantly alter textural characteristics in this experiment.

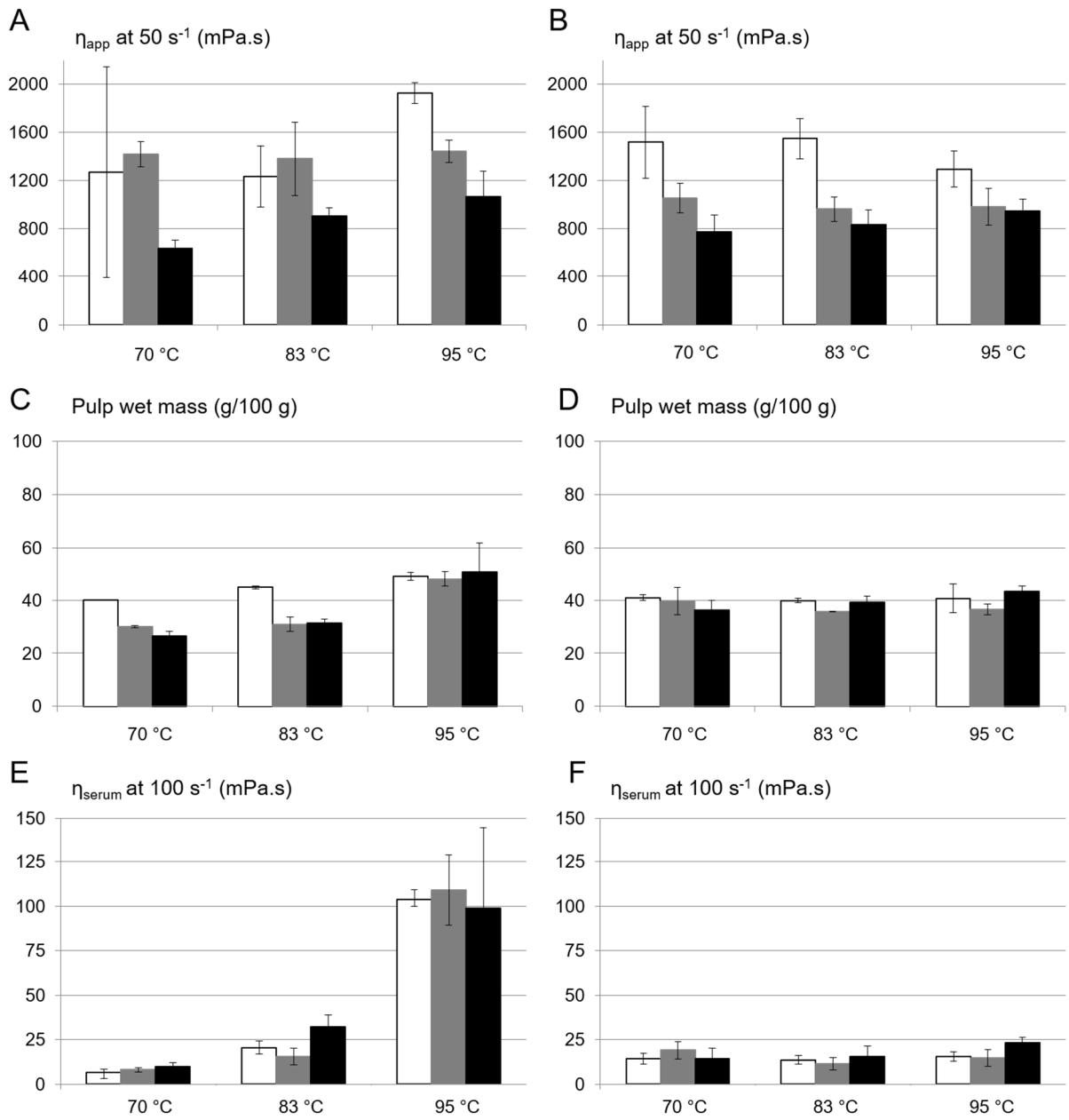

Fig. 1. Apparent puree viscosity at 50 s^{-1} (A, B), pulp wet mass (C, D) and serum viscosity at 100 s^{-1} (E, F) for purees obtained with different temperatures and grinding speeds for T1 (A, C, E) and T6 (B, D, F). White bars represent purees ground at 300 rpm, grey bars purees ground at 1000 rpm and black bars purees ground at 3000 rpm.

3.2. Determinants of apple puree's texture

3.2.1. Particle size distribution

For T1 and T6, particle size decreased with increased grinding speed (Fig. 2). This observation was correlated with puree's viscosity (Fig. 3A), which also decreased with grinding.

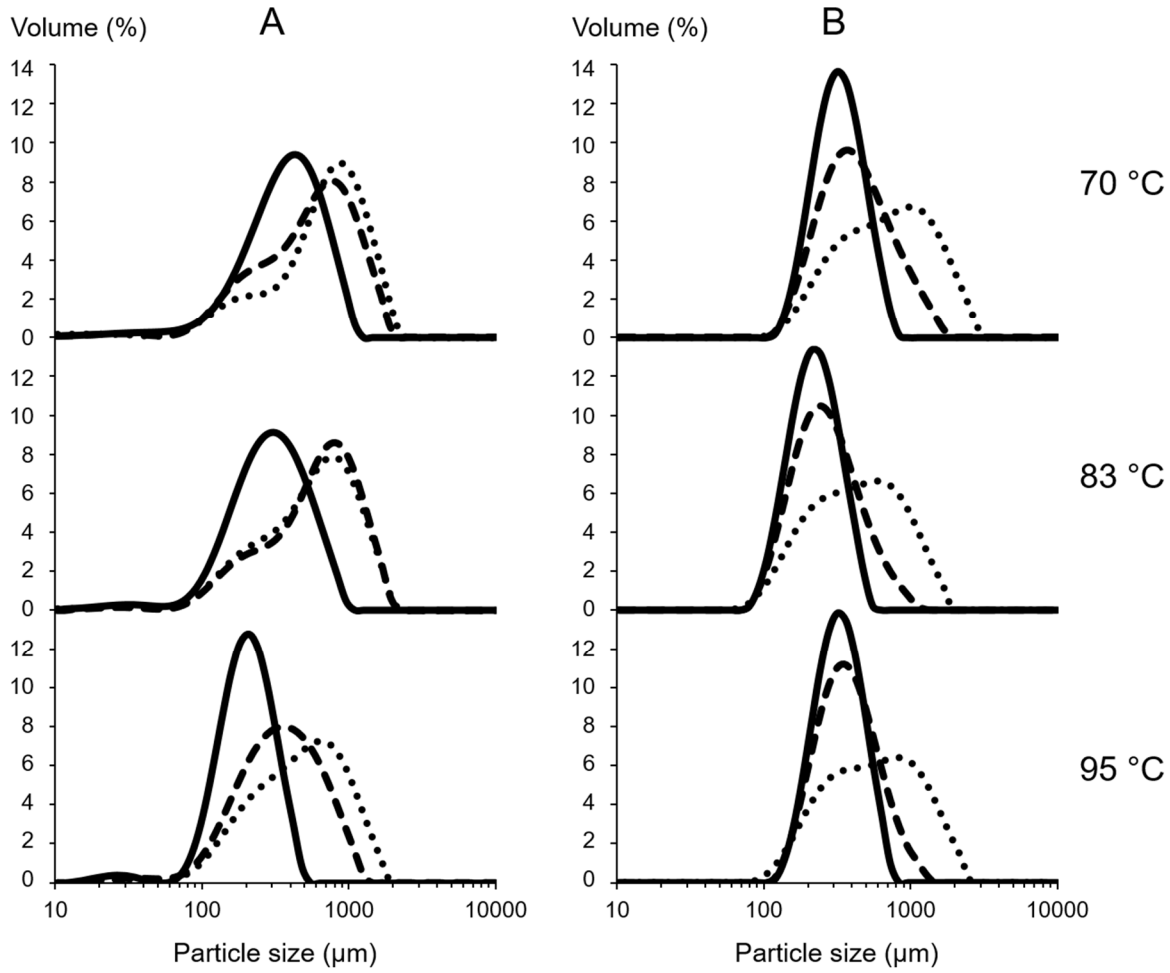

Fig. 2. Particle size distribution of purees obtained with different temperatures and grinding speeds for T1 (A) and T6 (B). Dotted lines represent purees ground at 300 rpm, dashed lines purees ground at 1000 rpm, and continuous lines purees ground at 3000 rpm.

For T1, particle size was also influenced by temperature (Fig. 2A). Purees prepared at low grinding speeds (300 and 1000 rpm) and moderate temperatures (70 and 83 °C) showed a bimodal distribution with the main peak around 950 µm and a shoulder, indicative of smaller particles. After grinding at 3000 rpm, particles showed a monomodal distribution around 480

317 µm at 70 °C and 360 µm at 83 °C. Particle size distributions for purees heated at 95 °C were
318 more narrow and exhibited smaller sizes at all grinding speeds: 630 µm, 315 µm and 210 µm
319 for purees ground at 300, 1000 and 3000 rpm, respectively. Since apple cells are around 200
320 µm in size (Khan & Vincent, 1990; Leverrier et al., 2016), only purees produced at 95 °C and
321 3000 rpm led to individualised cells for T1. Although these purees showed the smallest
322 particle sizes, they were more viscous than purees prepared at lower temperatures, even at the
323 same grinding speed (Fig. 1A). In this sense, grinding alone cannot account for the puree's
324 texture.
325 For T6 (Fig. 2B), particle size depended only on grinding speed (Supplementary Table S1).
326 Whereas purees ground at 300 rpm showed a prominent peak with a small shoulder, purees
327 prepared with grinding speeds of 1000 and 3000 rpm presented large quantities of individual
328 cells at all temperatures tested. Even though the same procedures produced smaller particles
329 than T1, this did not always result in less viscous purees (Fig. 1B).
330

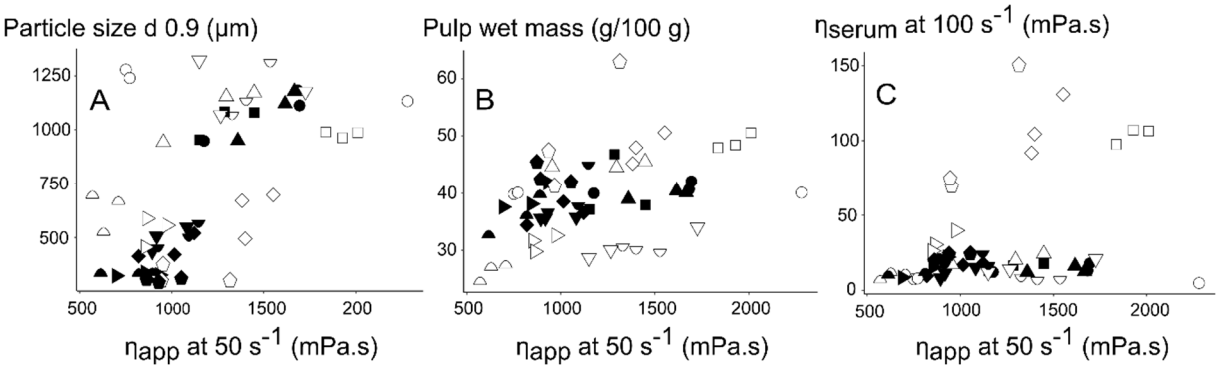

331

332 **Fig. 3.** Scatterplots of particle size (d 0.9) in the puree (A), pulp wet mass (B) and serum
333 viscosity at 100 s^{-1} (C) as a function of apparent puree viscosity at 50 s^{-1}. Empty symbols
334 represent samples for T1 and filled symbols samples for T6. 70 °C, 300 rpm (circle); 70 °C,
335 1000 rpm (half-circle downwards); 70 °C, 3000 rpm (half-circle upwards); 83 °C, 300 rpm
336 (triangle); 83 °C, 1000 rpm (triangle with the apex pointing downwards); 83 °C, 3000 rpm

337 (triangle with the apex pointing to the right); 95 °C, 300 rpm (square); 95 °C, 1000 rpm
338 (diamond); 95 °C, 3000 rpm (pentagon).
339
340 *3.2.2. Pulp wet mass, water retention capacity and cell wall porosity*
341 PWM for T1 (Fig. 1C) was similar for purees obtained at 70 and 83 °C. On the other hand,
342 this value was significantly increased in in purees prepared at 95 °C. Since the pulp's WRC
343 (Fig. 4A) were also higher for purees heated at 95 °C, higher temperatures probably increased
344 cell wall degradation, suggesting that the cell wall was retaining water. A similar observation
345 was reported previously with heat-treated dietary fibres (Guillon, Barry, & Thibault, 1992)
346 and apple cell wall material (Müller & Kunzek, 1998).
347 Grinding speed did not induce significant differences (Supplementary Table S1). The higher
348 PWM of the purees obtained at 300 rpm (70 and 83 °C) resulted from intact cell clusters,
349 which did not pack during centrifugation. These cell clusters are more rigid and occupy more
350 volume (Leverrier et al., 2016; Lopez-Sanchez, Chapara, Schumm, & Farr, 2012).
351 For T6, the temperature did not affect the PWM values (Fig. 1D). It is plausible that the fruit
352 maturation damaged the cell wall structure, limiting the impact of temperature. Grinding
353 showed a slightly significant impact on PWM for T6 but no trend could be observed. Overall,
354 the PWM was not significantly altered with storage. However, the PWM of aged cells seemed
355 to be higher when moderate temperatures (70 and 83 °C) and higher grinding speeds (1000
356 and 3000 rpm) were applied. The results obtained under these conditions were similar to T1
357 subjected to low grinding (300 rpm) or high temperature (95 °C). This result is supported by
358 the pulp's WRC (Fig. 4A) and could be explained by cell walls' porosity.
359 The T_2 relaxation times (Fig. 4B) showed water mobility distribution in the rehydrated pulp
360 AIS. For these types of experiments, longer T_2 relaxation values are indicative of greater
361 water mobility. This relationship can be roughly linked to the meso-porosity of the material
362 since an increase in T_2 relaxation times involve, among others, an increase in average pore

size (Meng & Ragauskas, 2014). For T1, five T_2 relaxation domains were identified. In contrast, only four domains were detected in T6. These domains were slightly more narrow, particularly at the two highest temperatures, including a relative T6 sample "homogenisation". The slowest water mobility centred on a T_2 value of about 4 ms, corresponding to pore sizes ranging between 5 and 7.5 nm (Barron et al., 2021), could be associated with water molecules involved in strong interaction with macromolecules. These values tended to decrease with increased temperature, indicating reduced pore size with higher temperatures. Environments with higher relaxation times (45–340 ms) all tended to increase with temperature. This observation is partly due to an increase in pore size of 15-120 nm with temperature and accounts for augmented WRC and PWM values. In general, higher T_2 relaxation times were observed in aged cells, indicating more porous cell walls and higher PWM. The exact values are presented in Supplementary Table S2.

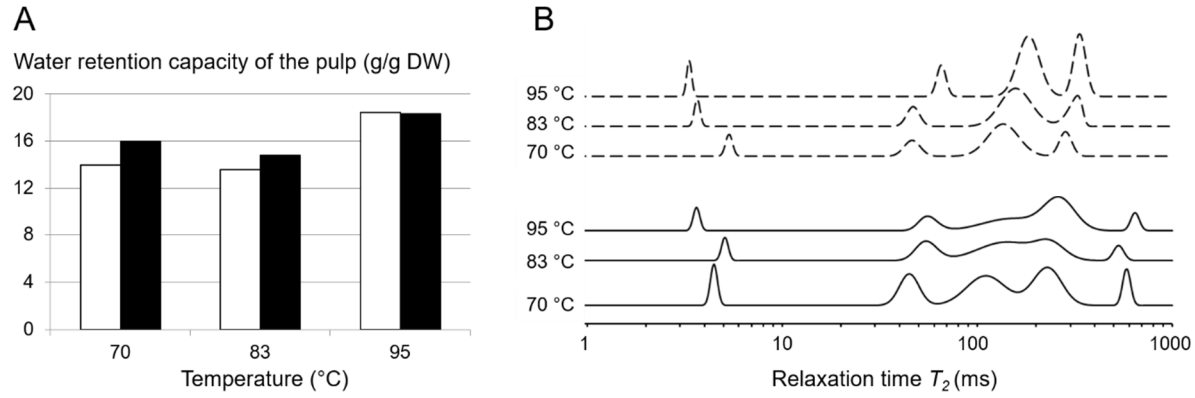

Fig. 4. Water retention capacity of the pulp (A) and relaxation times T_2 (B) for purees obtained at different temperatures and ground at 3000 rpm for T1 (white bars or continuous lines) and T6 (black bars or dashed lines).

Similar results were obtained with fresh purees (data not shown). However, other measurements, such as Simons' stain or NMR cryoporometry (Meng & Ragauskas, 2014), should be conducted to confirm the impact of temperature and storage on cell wall porosity.

Although the T1 purees prepared at higher temperatures exhibited smaller particle sizes, the purees were slightly more viscous (Fig. 1A). This result was probably due to the higher PWM values being correlated with more viscous purees (Fig. 3B). Additionally, while the T6 particles were significantly smaller (Supplementary Table S1), the purees' textural characteristics (apparent viscosity, yield stress, G′ and G″) were similar for T1 and T6. The higher PWM values in the older apples may have a smoothing effect on particle size. These results demonstrate the complex interactions between different texture determinants. Furthermore, altering these interactions by mechanical or thermal treatments can influence the puree texture.

3.2.3. Serum viscosity

Serum viscosity was significantly altered by temperature increase for T1 (Fig. 1E) but not for T6 (Fig. 1F). This effect was especially apparent for T1, in which the colour of the sera was more intense with increased grinding speed (Supplementary Fig. S3). This result might be due to small particle fragments in the serum. However, this did not alter serum viscosity since the grinding speed had no significant effect on this parameter. Overall, the storage duration did not significantly modify serum viscosity (Supplementary Table S1). It should be pointed out that the interaction between storage duration and temperature had a major impact, with T1 displaying lower serum viscosity values at 70 °C and impressively higher values at 95 °C than T6.

The purees' serum viscosity was found to be poorly correlated with their apparent viscosity (Fig. 3C). Additionally, serum viscosity did not vary significantly between the samples, except for T1 purees heated at 95 °C. These high serum viscosities might modify the sensory perception of consistency, resulting in a smoother texture in the mouth (Espinosa-Munoz, Symoneaux, Renard, Biau, & Cuvelier, 2012).

409 *3.3. Relation between process conditions and puree's texture*

410

411 Principal component analysis (PCA, Fig. 5) was conducted with textural characteristics
412 (apparent viscosity; yield stress; G′; G″), and possible determinants of puree's texture (particle
413 size; PWM, i.e. the amount of liquid phase bound by insoluble particles; serum viscosity) for
414 T1 and T6 were evaluated. Together, the first two principal components (PC1 and PC2)
415 explained more than 80% of the total variance. Yield stress, G′ and G″ were grouped at PC1,
416 together with particle size, indicating a strong dependence. T1 samples (Fig. 5B) were more
417 variable than T6 since they were more dispersed in the sample map. In conclusion, the impact
418 of processing on the puree's texture and its determinants was reduced by prolonged post-
419 harvest storage. Indeed, NMR relaxation experiments (Fig. 4B) and previous results (Buergy
420 et al., 2020) confirmed this conclusion.
421 T1 samples produced at 70 and 83 °C were placed together at PC1, while purees prepared at
422 95 °C were explained by PC2. This result led to two extremes, one at PC1 that accounted for
423 samples ground at 300 rpm and heated at moderate temperatures (70 and 83 °C) and one at
424 PC2, samples heated at 95 °C.
425 Samples were separated according to the grinding speed along PC1 (Fig. 5B). Thus, large
426 particles were related to high yield stress, G′ and G″. Cell clusters deform less easily than
427 individual cells and occupy more volume in the puree, consequently increasing the
428 rheological characteristics (Leverrier et al., 2016; Lopez-Sanchez et al., 2012). Moreover,
429 PWM and serum viscosity were placed near PC2 and perpendicular to the parameters
430 mentioned above. These results suggest that the two input variables temperature and grinding,
431 produce different effects.
432 Indeed, in the sample map (Fig. 5B), PC2 separated T1 purees produced at 95 °C, which were
433 characterised by high PWM and high serum viscosities (Fig. 1C and E), from T1 purees
434 produced at moderate temperatures (70 °C and 83 °C). On the other hand, the T6 purees were

intermediate. Apparent viscosity was less well explained in the PCA and stood alone between PC1 and PC2. This observation indicated some co-dependence with particle size (along PC1) and PWM and serum viscosity (along PC2). Hence, texture formation was influenced by grinding, a step that highly affected particle size, and temperature, which facilitated tissue separation in synergy with grinding, increased PWM, and serum viscosity.

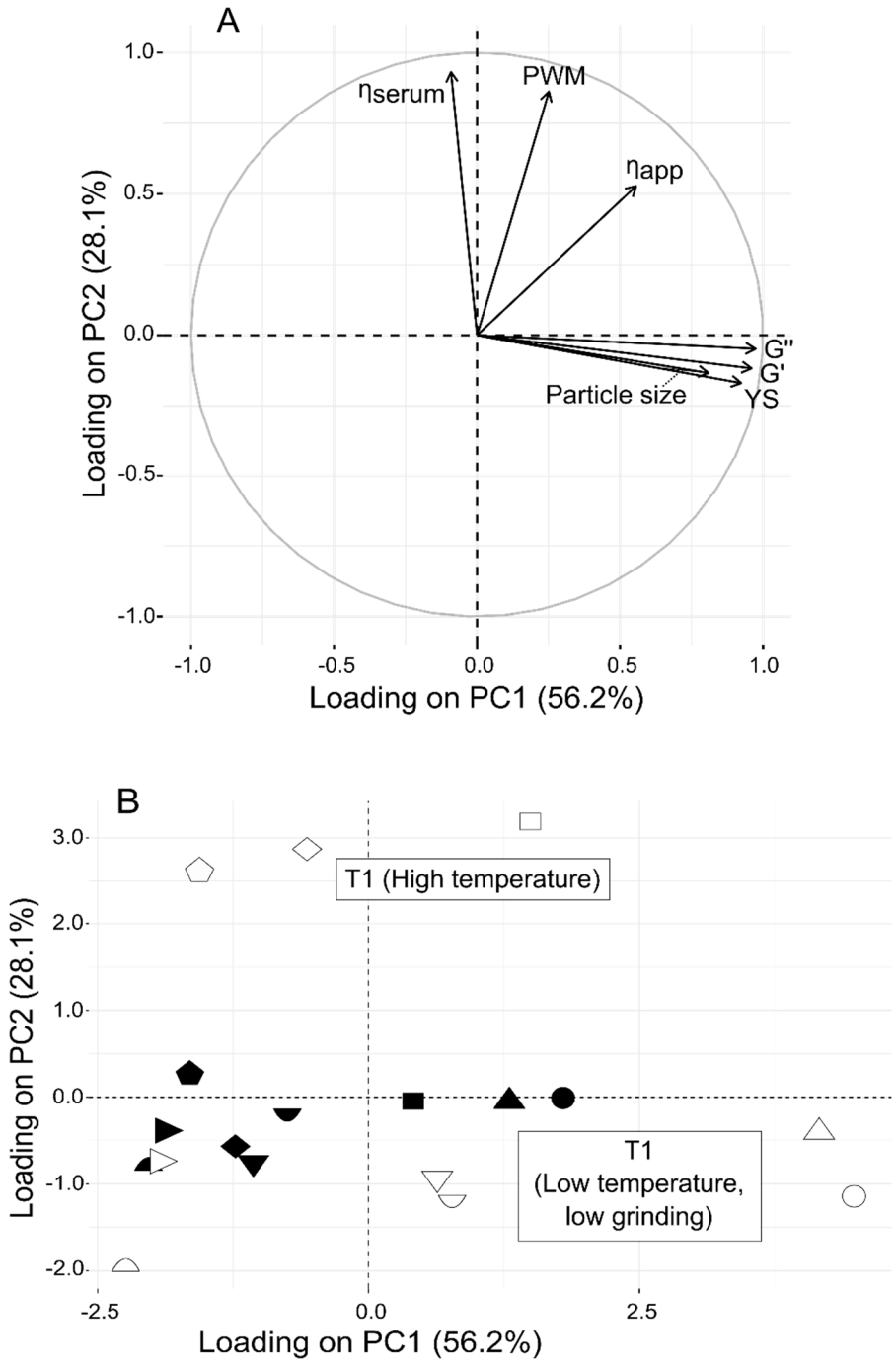

Fig. 5. Principal component analysis (PCA) of rheological characteristics (η_{app}: apparent puree viscosity at 50 s^{-1}, YS: yield stress, G′ and G″: puree's storage and loss modulus, respectively, at an angular frequency of 10 rad/s) and texture determinants (Particle size: particle size d 0.9, PWM: pulp wet mass, η_{serum}: serum viscosity at 100 s^{-1}) of purees prepared with apples stored for one and six months before processing. Correlation circle of variables loadings on PC1 and PC2 (A). Sample maps of scores on PC1 and PC2 (B). For more legibility, PCA was conducted on the mean value of three replications as the same patterns were obtained as for PCA with all values. Empty symbols represent samples for T1 and filled symbols samples for T6. 70 °C, 300 rpm (circle); 70 °C, 1000 rpm (half-circle downwards); 70 °C, 3000 rpm (half-circle upwards); 83 °C, 300 rpm (triangle); 83 °C, 1000 rpm (triangle with the apex pointing downwards); 83 °C, 3000 rpm (triangle with the apex pointing to the right); 95 °C, 300 rpm (square); 95 °C, 1000 rpm (diamond); 95 °C, 3000 rpm (pentagon).

3.4. Serum pectins can help to explain texture determinants

Mechanical and thermal treatment act synergistically during puree processing, affecting texture determinants to different extents because temperature favours pectin degradation and solubilisation (Sila et al., 2009). The detailed structural and compositional characterisation of the pectins solubilised during processing (serum pectins) could provide insight into the chemical processes that occur during apple processing. This knowledge could help elucidate the complex interactions between texture determinants and lead to a specific puree's texture, depending on post-harvest storage. Serum pectins were solubilised from the middle lamella or the primary cell wall (Sila et al., 2009), thus facilitating tissue fragmentation (i.e., reduced particle size) or increasing porosity and consequently the pulp's WRC (i.e., increased PWM). The amount of solubilised pectins would, in turn, explain serum viscosity.

3.4.1. Chemical composition of serum pectins

For T1, the amount and chemical composition of serum pectins was significantly altered by temperature but not by grinding (Table 1). Serum AIS values were significantly increased with elevated temperature, indicating improved pectin solubilisation from the cell wall and middle lamella. This effect might weaken the cell wall structure and intercellular adhesion, facilitating cell separation during grinding at elevated temperatures. Previous studies showed that heating raw apple, carrot or broccoli tissue before grinding aided separation (Day et al., 2010; Lopez-Sanchez et al., 2011; Müller & Kunzek, 1998) but the results were not corroborated with pectin analysis. Increased pectin solubilisation might also increase the pore sizes in the cell wall (Fig. 4B), leading to improved WRC of the pulp (Fig. 4A) and PWM (Fig. 1C). The amount of solubilised pectins was also correlated with the temperature-dependent increase in serum viscosity (Fig. 6A). Starch solubilisation might additionally increase serum viscosity. The amount of starch in the serum significantly increased with temperature and slightly with grinding speed until reaching a concentration of about 13 g/L at 95 °C and 3000 rpm. Considering that the gelatinisation temperature of starch in excess water is around 60 °C, temperatures above 70 °C might solubilise starch better (Singh, Inouchi, & Nishinari, 2005). Increased grinding also seemed to enhance starch solubilisation and was probably due to increased cell wall rupture. Although amylose gels at less than 10 g/L (Doublier & Choplin, 1989) and a 20 g/L amylopectin solution provides a viscosity increase of 5 mPa.s (Matignon et al., 2014), these relatively low concentrations cannot account for the high serum viscosity increase.

The GalA content in serum AIS also increased with temperature, confirming improved pectin solubilisation at high temperatures. The GalA/rhamnose ratio estimated the proportion of HG to RG I pectins. It was not altered either by temperature or by grinding, indicating that HG and RG I pectins were similarly solubilised. Although arabinan side chains are generally more susceptible to temperature than galactans (Green, 1967; Thibault et al., 1993), the

galactan/arabinan ratio decreased with increasing temperature. Pectin RG I fractions rich in arabinans thus seemed to be more tightly bound to the cell wall and required more degradation for solubilisation. The ratio of (arabinose+galactose)/rhamnose also decreased with increasing temperature, revealing attenuated RG I side chain branching. Since RG I side chains were shown to be linked to the cellulose-xyloglucan network in the cell wall (Popper & Fry, 2005; Zykwinska, Ralet, Garnier, & Thibault, 2005), pectins seemed to be less attached and thus more susceptible to solubilisation during processing.

All serum pectins were highly methylated, and the DM was not affected by temperature (results not shown), attesting limited impact of PME activity during apple processing.

Compared to T1, the amount and composition of serum pectins for T6 were less affected by thermomechanical processes (Table 1) during puree production. This observation could be because endogenous enzymes already degraded pectins. The serum AIS content at 70° C was higher for T6 than T1 but remained constant at any temperature, thus accounting for T6's constant serum viscosity regardless of the processing conditions (Fig. 1F). Starch was not detected. The AIS composition of serum pectins was stable for T6, whatever the grinding or temperature. As an exception, the galactan/arabinan ratio was slightly decreased with increased temperature, but the values were less dispersed than for T1 and the overall (arabinose+galactose)/rhamnose ratio was not modified. Compared to T1, the latter ratio was less critical and indicated reduced RG I side chain branching in T6 serum pectins. This substantial decrease in RG I side chains (i.e., arabinose and galactose) probably contributed to the higher relative GalA content in the T6 samples. Concerning T1, the HG to RG I ratio, expressed as GalA/rhamnose, was not altered by temperature or grinding. However, this ratio showed that, although the GalA content was higher for T6, more RG I was extracted, especially with grinding. This result may be due to reduced RG I side chains, leading to a weakened cell wall structure, as explained before. As observed by Nara et al. (2001) or Pena and Carpita (2004), reduced RG I side chains were probably linked to reduced cell adhesion.

520 Indeed, cell separation was easy for T6 and purees prepared with aged apples showed
521 significantly smaller particles (Supplementary Table S1). Additionally, grinding generated
522 similar particle sizes independent of temperature. As previously stated by Buergy et al.
523 (2020), ageing facilitated cell separation for T6. As hypothesised before, the weakening of the
524 cell wall in aged apples probably increased cell wall porosity (Fig. 4B), leading to increased
525 WRC (Fig. 4A) and PWM (Fig. 1D).
526 Since raw apples also displayed RG I side chain loss, GalA increase and more RG I during
527 post-harvest storage (Supplementary Table S3), it is plausible that storage could be exploited
528 for producing a desired puree's texture.
529

530 **Table 1.** AIS yield, composition, and macromolecular characteristics of serum pectins, followed by Kruskal-Wallis *H*- and *P*-values.

Storage (months)	Temp. (°C)	Grinding (rpm)	AIS (mg/g FW)	Starch (mg/g FW)	GalA (mg/g AIS)	$\frac{\text{GalA}}{\text{Rha}}$	$\frac{\text{Ara + Gal}}{\text{Rha}}$	$\frac{\text{Gal}}{\text{Ara}}$	$\overline{M}_w \times 10^3$ (g/mol)	$\overline{[\eta]}_z$ (mL/g)	d_{happ} (g nm^3/mol)
1	70	300	0.9	0.1	527	73	24	1.4	311	1903	0.8
		1000	1.1	0.2	556	94	24	1.4	545	1869	0.8
		3000	1.6	0.5	470	60	26	1.3	480	1811	0.8
	83	300	2.1	0.4	554	117	22	1.2	493	1609	0.9
		1000	1.7	0.4	539	88	25	1.2	522	1760	0.9
		3000	3.0	0.6	543	93	25	1.0	455	1783	0.8
	95	300	5.3	0.5	646	74	17	0.8	406	1229	1.2
		1000	5.8	1.0	602	82	21	0.8	425	1272	1.2
		3000	6.2	1.3	577	81	22	0.8	409	1268	1.2
6*	70	300	2.1	ND	683	52	8	1.1	157	510	3.0
		1000	1.8	ND	593	26	6	1.2	188	488	3.1
		3000	3.0	ND	605	30	7	1.0	273	579	2.6
	83	300	2.4	ND	663	48	7	1.0	166	583	2.6
		1000	2.5	ND	601	26	6	0.9	204	650	2.3
		3000	3.1	ND	605	27	6	1.0	229	620	2.4
	95	300	3.9	ND	689	67	10	0.8	159	507	3.0
		1000	3.4	ND	636	31	6	0.8	217	607	2.5
		3000	4.5	ND	619	28	6	0.8	250	636	2.4
PSD			0.8	0.5	49	28	3	0.1	50	162	0.1

1	Temperature H	20.9	10.6	9.6	3.4	7.5	22.6	5.5	18.6	18.3
	Temperature P	**<0.001**	**0.005**	**0.008**	0.184	**0.023**	**<0.001**	0.064	**<0.001**	**0.000**
	Grinding H	1.1	3.3	2.0	0.4	3.0	0.5	4.8	1.0	1.2
	Grinding P	0.572	0.190	0.361	0.804	0.220	0.798	0.089	0.614	0.556
6*	Temperature H	6.0	-	1.7	1.2	1.2	7.2	2.4	3.2	4.6
	Temperature P	0.051	-	0.430	0.561	0.561	**0.027**	0.301	0.202	0.099
	Grinding H	1.7	-	5.6	5.6	5.6	0.1	2.4	2.5	0.3
	Grinding P	0.430	-	0.061	0.061	0.061	0.957	0.301	0.288	0.875
Storage H		0.3	-	10.7	15.7	19.7	2.4	19.1	19.7	11.9
Storage P		0.596	-	**0.001**	**<0.001**	**<0.001**	0.121	**<0.001**	**<0.001**	**0.001**

* Only one repetition per sample.

The ratio GalA/Rha estimated the relative amount of HG versus RG I, (Ara+Gal)/Rha estimated RG I branching and Gal/Ara the proportion of RG I side chains. Ratios were calculated using the yields of galacturonic acid (GalA) and neutral sugars arabinose (Ara), galactose (Gal) and rhamnose (Rha) content, expressed in mg/g AIS (Supplementary Table S4). AIS and chemical composition of serum pectins were corrected for the starch content. PSD: Pooled standard deviations; ND: Not detected; FW: Fresh weight (serum); AIS: Alcohol insoluble solids; $\overline{M}_w$: Weight-average molar mass; $\overline{[\eta]}_z$: z-average intrinsic viscosity; d_{happ}: Apparent molecular density, calculated as $\overline{M}_w/(\frac{4}{3}\cdot\pi\cdot\overline{R}_{hz}(v)^3)$ with $\overline{R}_{hz}(v)$: z-average viscometric hydrodynamic radius. Macromolecular characteristics were taken at the apex of the main peak.

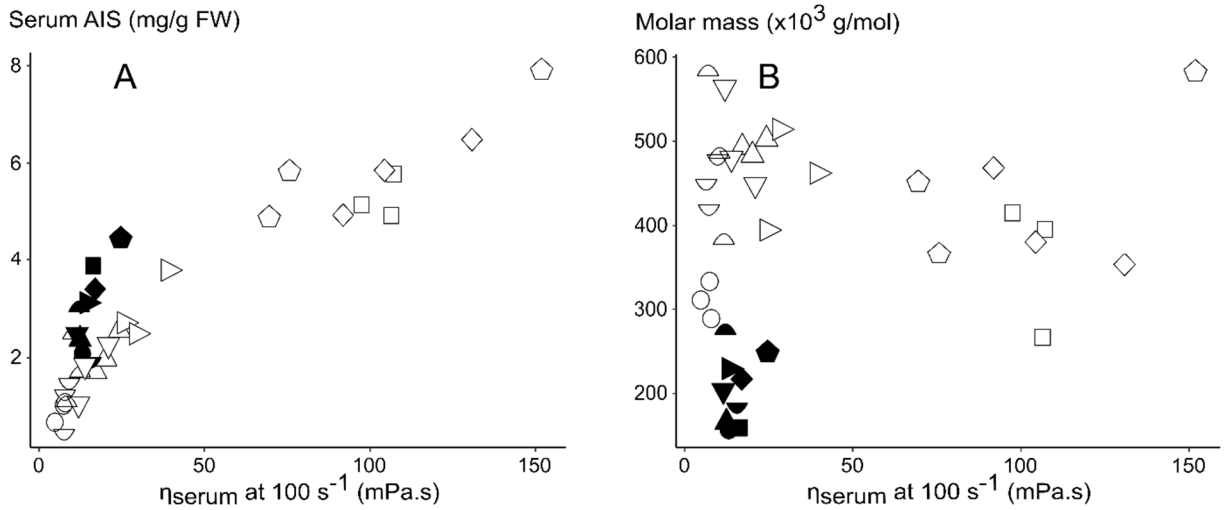

Fig. 6. Scatterplots of serum viscosity at 100 s^{-1} against serum AIS (A) and molar mass of serum pectins at the apex of the main peak (B). Empty symbols represent samples for T1 and filled symbols samples for T6. 70 °C, 300 rpm (circle); 70 °C, 1000 rpm (half-circle downwards); 70 °C, 3000 rpm (half-circle upwards); 83 °C, 300 rpm (triangle); 83 °C, 1000 rpm (triangle with the apex pointing downwards); 83 °C, 3000 rpm (triangle with the apex pointing to the right); 95 °C, 300 rpm (square); 95 °C, 1000 rpm (diamond); 95 °C, 3000 rpm (pentagon).

3.4.2. Macromolecular characteristics of serum pectins

Macromolecular characteristics of soluble serum pectins give information about their molecular structure and density. For T1, molar mass (Table 1) was not significantly altered by temperature but showed an overall decrease when higher temperatures were applied. For T6, molar mass was not altered by processing, but values were significantly lower than for T1. The molar mass distributions of serum pectins (Fig. 7) are presented for samples prepared at 3000 rpm and different temperatures. For T1 purees (Fig. 7A) processed at moderate temperatures (70 °C and 83 °C), the main fraction of serum pectin eluted at the same elution volume (~19 mL), whereas the main peak was shifted to higher elution volumes after heating at 95 °C. This result indicated a smaller pectin size for the samples obtained at 95 °C. A

558 second peak eluting at higher elution volumes (~25 mL), which represented smaller pectin
559 fractions, was also present, and its proportion decreased with increased temperature.
560 However, $\overline{M}_w$ (90–105 x 10^3 g/mol) and $\overline{R}_{hz}(v)$ (10–16 nm) were similar in all samples and
561 could not be differentiated. For T6 (Fig. 7B), processing temperature did not affect the serum
562 pectins' macromolecular size. Compared with T1, the main peak of all pectin chromatograms
563 was shifted to higher elution volumes, and the second peak was smaller, indicating pectin
564 degradation during storage as observed before (Buergy et al., 2020). Hence, both increased
565 temperature (95 °C, for T1) and post-harvest storage induced pectin degradation, thus
566 favouring pectin solubilisation. A reduction in RG I side chains weakened the cell wall
567 structure, leading to reduced cell adhesion and more porous cell walls. However, no trend was
568 observed between serum viscosity and molar mass (Fig. 6B).
569 It has been reported that pectin conformation can significantly impact serum viscosity (Diaz,
570 Anthon, & Barrett, 2009). Herein, intrinsic viscosity was significantly affected by temperature
571 increase (Table 1), leading to reduced values at 95 °C despite higher pectin concentrations.
572 Lower intrinsic viscosities at 95 °C for comparable molar mass at 70 and 83 °C indicted a
573 more compact pectin structure. This observation was confirmed by $\overline{R}_{hz}(v)$ conformation plots
574 (Supplementary Fig. S4) and the apparent polymer density d_{happ} (Table 1). The latter was
575 similar at 70 and 83 °C but significantly higher for 95 °C. Intrinsic viscosity was significantly
576 lower for T6, roughly half that of T1, whereas d_{happ} increased by more than 2-fold. Since
577 serum pectins in purees from aged apples have more GalA and less arabinose and galactose
578 (Table 1), this higher density could result from more properly folded pectins because of
579 reduced steric hindrance. Although the conformation of serum pectins was altered, it could
580 not be linked to serum viscosity (data not shown).
581 Grinding had no impact on the macromolecular characteristics of the T1 serum pectins. In
582 contrast, molar mass and intrinsic viscosity of T6 pectins increased with grinding, although

this trend was not statistically significant. Macromolecular characteristics of soluble pectins extracted from raw apples showed the same trend as serum pectins during post-harvest storage (i.e., smaller molar mass and intrinsic viscosity but higher d_{happ}) (Supplementary Table S3).

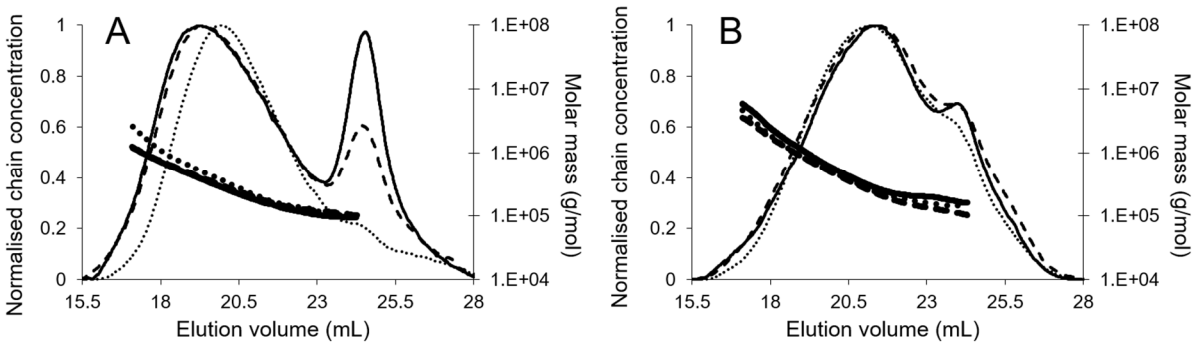

Fig. 7. Normalised chain concentration and molar mass versus elution volume of serum pectins for T1 (A) and T6 (B) for purees prepared at 70 °C (continuous lines), 83 °C (dashed lines) and 95 °C (dotted lines) and a grinding speed of 3000 rpm. The signal (mV) obtained by the differential refractive index detector was normalised by dividing all data points by the signal at the peak's apex.

3.4.3. Mechanisms of pectin degradation during processing

At the natural pH of apples (~3.7), pectin degradation is minimal and might be due to either acid hydrolysis or β-elimination (Liu, Renard, Rolland-Sabaté, Bureau, & Le Bourvellec, 2021). For T1 (Table 1), serum pectins showed higher amounts of GalA and the RG I side chains arabinan and galactan were hydrolysed by temperature increase, which probably favoured the extractability of pectins from the cell wall. Moreover, T1 serum pectins showed reduced molar mass, macromolecular size and intrinsic viscosity (Table 1 and Fig. 7A) when temperature increased from 83 to 95 °C, attesting pectin degradation. To investigate the mechanisms leading to pectin degradation at 95 °C, NMR was used to detect β-elimination

products in serum pectins, since the 235 nm wavelength in the DAD signal after sample separation by HPSEC was not enough to detect β-elimination (data not shown). A small signal in the ^{1}H-NMR spectrum around 6 ppm indicated the presence of β-elimination products (Tjan et al., 1974). This signal was visible in the positive control and, slightly, in the serum AIS obtained from purees heated at 95 °C (Fig. 8). In conclusion, only little β-elimination occurred, even at 95 °C, and acid hydrolysis seemed to be the predominant reaction causing pectin degradation during apple processing.

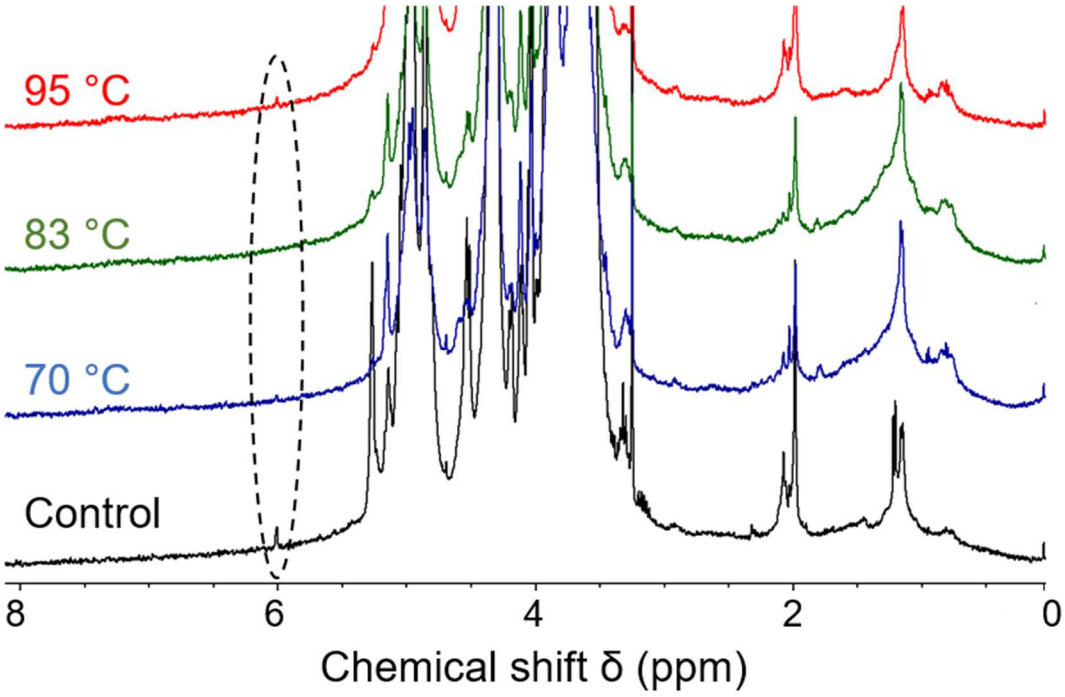

Fig. 8. ^{1}H-NMR spectra of control and serum pectins extracted from the purees at 3000 rpm with different temperatures for T1. The control (serum pectin 95 °C, 3000 rpm) was heated at 100 °C for 30 min at pH 6 to enhance β-elimination.

5. Conclusions

Both elevated temperature (95 °C) and apple maturation led to pectin degradation, resulting in facilitated tissue fragmentation during processing. This treatment affected particle size, an

important determinant of puree's texture, and other parameters such as PWM and serum viscosity. Since pectin and puree's structures were significantly altered by increasing temperature in fresh (T1) but not in older (T6) apples, the combination of storage duration and temperature had a significant impact. Although mechanical treatments were the predominant factor for texture formation, they did not alter the pectin composition or structure, in T1 or T6. The temperature had only a limited impact on the apple puree's texture. However, it strongly affected PWM and serum viscosity, which counteracted the effect of smaller particles produced by grinding. This study highlighted the importance of pectin analysis in explaining the impact of thermomechanical processes on puree's texture. A detailed characterisation of the pulp's cell wall composition and structure should be performed in future work. It would also be interesting to conduct detailed kinetics, over short periods of 5 to 15 min, at different temperatures and grinding speeds to precisely identify the moment structural alterations occur.

CRediT authorship contribution statement

Alexandra Buergy: Conceptualization, Investigation, Formal analysis, Data curation, Writing - original draft. **Agnès Rolland-Sabaté:** Conceptualization, Supervision, Validation, Writing - review & editing. **Alexandre Leca:** Conceptualization, Investigation, Supervision, Writing - review & editing. **Xavier Falourd:** Investigation, Formal analysis, Writing - review & editing. **Loïc Foucat:** Investigation, Formal analysis, Writing - review & editing. **Catherine M. G. C. Renard:** Conceptualization, Funding acquisition, Project administration, Validation, Writing - review & editing.

Declaration of competing interest

Declarations of interest: none.

Acknowledgements

This work was carried out as part of "Interfaces" flagship project, publicly funded through ANR (the French National Agency) under the "Investissements d´avenir" program with the reference ANR-10-LABX-001-01 Labex Agro and coordinated by Agropolis Fondation under the reference ID 1603-001. HPSEC-MALLS studies were supported by Platform 3A facilities, funded by the European Regional Development Fund, the French Ministry of Research, Higher Education and Innovation, the Provence Alpes Côte d'Azur region, the Departmental Council of Vaucluse and the Urban Community of Avignon. NMR analyses were realised on the BIBS instrumental platform (http://www.bibs.inra.fr/bibs_eng/, UR1268 BIA, IBiSA, Phenome-Emphasis-FR ANR-11-INBS-0012).

References

Anthon, G. E., Diaz, J. V., & Barrett, D. M. (2008). Changes in pectins and product consistency during the concentration of tomato juice to paste. *Journal of Agricultural and Food Chemistry, 56*(16), 7100-7105.

Barron, C., Devaux, M.-F., Foucat, L., Falourd, X., Looten, R., Joseph-Aimé, M., Durand, S., Bonnin, E., Lapierre, C., Saulnier, L., Rouau, X., & Guillon, F. (2021). Enzymatic degradation of maize shoots: Monitoring of chemical and physical changes reveals different saccharification behaviors. *Biotechnology for Biofuels, 14(1)*.

671 Blumenkrantz, N., & Asboe-Hansen, G. (1973). New method for quantitative-determination
672 of uronic acids. *Analytical Biochemistry, 54*(2), 484-489.
673 Box, G. E. P., Hunter, W. G., & Hunter, J. S. (1978). *Statistics for Experimenters: An*
674 *Introduction to Design, Data Analysis, and Model Building*. New York: John Wiley
675 and Sons.
676 Buergy, A., Rolland-Sabaté, A., Leca, A., & Renard, C. M. G. C. (2020). Pectin modifications
677 in raw fruits alter texture of plant cell dispersions. *Food Hydrocolloids, 107*, 105962.
678 Carpita, N. C., & Gibeaut, D. M. (1993). Structural models of primary-cell walls in flowering
679 plants - Consistency of molecular-structure with the physical-properties of the walls
680 during growth. *Plant Journal, 3*(1), 1-30.
681 Christiaens, S., Mbong, V. B., Van Buggenhout, S., David, C. C., Hofkens, J., Van Loey, A.
682 M., & Hendrickx, M. E. (2012). Influence of processing on the pectin structure-
683 function relationship in broccoli puree. *Innovative Food Science & Emerging*
684 *Technologies, 15*, 57-65.
685 Day, L., Xu, M., Oiseth, S. K., Lundin, L., & Hemar, Y. (2010). Dynamic rheological
686 properties of plant cell-wall particle dispersions. *Colloids and Surfaces B:*
687 *Biointerfaces, 81*(2), 461-467.
688 Diaz, J. V., Anthon, G. E., & Barrett, D. M. (2009). Conformational changes in serum pectins
689 during industrial tomato paste production. *Journal of Agricultural and Food*
690 *Chemistry, 57*(18), 8453-8458.
691 Doublier, J. L., & Choplin, L. (1989). A rheological description of amylose gelation.
692 *Carbohydrate Research, 193*, 215-226.
693 Englyst, H., Wiggins, H. S., & Cummings, J. H. (1982). Determination of the non-starch
694 polysaccharides in plant-foods by gas-liquid-chromatography of constituent sugars as
695 alditol acetates. *Analyst, 107*(1272), 307-318.

696 Espinosa-Munoz, L., Symoneaux, R., Renard, C. M. G. C., Biau, N., & Cuvelier, G. (2012).
697 The significance of structural properties for the developent of innovative apple puree
698 textures. *LWT-Food Science and Technology, 49*(2), 221-228.
699 Espinosa, L., To, N., Symoneaux, R., Renard, C. M. G. C., Biau, N., & Cuvelier, G. (2011).
700 Effect of processing on rheological, structural and sensory properties of apple puree.
701 In G. Saravacos, P. Taoukis, M. Krokida, V. Karathanos, H. Lazarides, N. Stoforos, C.
702 Tzia & S. Yanniotis (Eds.), *11th International Congress on Engineering and Food*
703 (Vol. 1, pp. 513-520). Amsterdam: Elsevier Science Bv.
704 Green, J. W. (1967). The glycofuranosides. In M. L. Wolfrom & R. S. Tipson (Eds.),
705 *Advances in Carbohydrate Chemistry* (Vol. 21, pp. 95-142): Academic Press.
706 Guillon, F., Barry, J.-L., & Thibault, J.-F. (1992). Effect of autoclaving sugar-beet fibre on its
707 physico-chemical properties and its in-vitro degradation by human faecal bacteria.
708 *Journal of the Science of Food and Agriculture*, *60*(1), 69-79.
709 Jarvis, M. C. (1984). Structure and properties of pectin gels in plant-cell walls. *Plant Cell and*
710 *Environment, 7*(3), 153-164.
711 Khan, A. A., & Vincent, J. F. V. (1990). Anisotropy of apple parenchyma. *Journal of the*
712 *Science of Food and Agriculture, 52*(4), 455-466.
713 Kohn, R., & Luknár, O. (1977). Intermolecular calcium ion binding on polyuronates-
714 polygalacturonate and polyguluronate. *Collection of Czechoslovak Chemical*
715 *Communications, 42*, 731-744.
716 Kruskal, W. H., & Wallis, W. A. (1952). Use of ranks in one-criterion variance analysis.
717 *Journal of the American Statistical Association, 47*(260), 583-621.
718 Lahaye, M., Bouin, C., Barbacci, A., Le Gall, S., & Foucat, L. (2018). Water and cell wall
719 contributions to apple mechanical properties. *Food Chemistry, 268*, 386-394.

720 Le Bourvellec, C., Bouzerzour, K., Ginies, C., Regis, S., Ple, Y., & Renard, C. M. G. C.
721 (2011). Phenolic and polysaccharidic composition of applesauce is close to that of
722 apple flesh. *Journal of Food Composition and Analysis, 24*(4-5), 537-547.
723 Lê, S., Josse, J., & Husson, F. (2008). FactoMineR: An R package for multivariate analysis.
724 *Journal of Statistical Software, 25*(1), 1-18.
725 Leverrier, C., Almeida, G., Espinosa-Munoz, L., & Cuvelier, G. (2016). Influence of particle
726 size and concentration on rheological behaviour of reconstituted apple purees. *Food*
727 *Biophysics, 11*(3), 235-247.
728 Liu, X., Renard, C. M. G. C., Rolland-Sabaté, A., Bureau, S., & Le Bourvellec, C. (2021).
729 Modification of apple, beet and kiwifruit cell walls by boiling in acid conditions:
730 Common and specific responses. *Food Hydrocolloids, 112*, 106266.
731 Lopez-Sanchez, P., Chapara, V., Schumm, S., & Farr, R. (2012). Shear elastic deformation
732 and particle packing in plant cell dispersions. *Food Biophysics, 7*(1), 1-14.
733 Lopez-Sanchez, P., Nijsse, J., Blonk, H. C. G., Bialek, L., Schumm, S., & Langton, M.
734 (2011). Effect of mechanical and thermal treatments on the microstructure and
735 rheological properties of carrot, broccoli and tomato dispersions. *Journal of the*
736 *Science of Food and Agriculture, 91*(2), 207-217.
737 Matignon, A., Ducept, F., Sieffermann, J.-M., Barey, P., Desprairies, M., Mauduit, S., &
738 Michon, C. (2014). Rheological properties of starch suspensions using a rotational
739 rheometer fitted with a starch stirrer cell. *Rheologica Acta, 53*(3), 255-267.
740 Meng, X., & Ragauskas, A. J. (2014). Recent advances in understanding the role of cellulose
741 accessibility in enzymatic hydrolysis of lignocellulosic substrates. *Current Opinion in*
742 *Biotechnology, 27*, 150-158.
743 Moelants, K., Cardinaels, R., Jolie, R., Tina, V., Buggenhout Sandy, V., Zumalacarregui, L.,
744 van Loey, A., Moldenaers, P., & Hendrickx, M. (2012). Relation between particle

properties and rheological characteristics of carrot-derived suspensions. *Food and Bioprocess Technology, 6*.

Moelants, K. R. N., Cardinaels, R., Jolie, R. P., Verrijssen, T. A. J., Van Buggenhout, S., Van Loey, A. M., Moldenaers, P., & Hendrickx, M. E. (2014). Rheology of concentrated tomato-derived suspensions: Effects of particle characteristics. *Food and Bioprocess Technology*.

Mohnen, D. (2008). Pectin structure and biosynthesis. *Current Opinion in Plant Biology, 11*(3), 266-277.

Müller, S., & Kunzek, H. (1998). Material properties of processed fruit and vegetables - I. Effect of extraction and thermal treatment on apple parenchyma. *Zeitschrift für Lebensmittel-Untersuchung und -Forschung, 206*(4), 264-272.

Nara, K., Kato, Y., & Motomura, Y. (2001). Involvement of terminal-arabinose and -galactose pectic compounds in mealiness of apple fruit during storage. *Postharvest Biology and Technology, 22*(2), 141-150.

Ndeh, D., Rogowski, A., Cartmell, A., Luis, A. S., Baslé, A., Gray, J., Venditto, I., Briggs, J., Zhang, X., Labourel, A., Terrapon, N., Buffetto, F., Nepogodiev, S., Xiao, Y., Field, R. A., Zhu, Y., O'Neill, M. A., Urbanowicz, B. R., York, W. S., Davies, G. J., Abbott, D. W., Ralet, M.-C., Martens, E. C., Henrissat, B., & Gilbert, H. J. (2017). Complex pectin metabolism by gut bacteria reveals novel catalytic functions. *Nature, 544*(7648), 65-70.

Pena, M. J., & Carpita, N. C. (2004). Loss of highly branched arabinans and debranching of rhamnogalacturonan I accompany loss of firm texture and cell separation during prolonged storage of apple. *Plant Physiology, 135*(3), 1305-1313.

768 Popper, Z. A., & Fry, S. C. (2005). Widespread occurrence of a covalent linkage between
769 xyloglucan and acidic polysaccharides in suspension-cultured angiosperm cells.
770 *Annals of Botany, 96*(1), 91-99.
771 R Core Team. (2018). R: A language and environment for statistical computing. *R*
772 *Foundation for Statistical Computing*, Vienna, Austria. https://www.R-project.org/.
773 (Accessed 14 March 2018).
774 Rao, M. A. (1992). The structural approach to rheology of plant food dispersions. *Revista*
775 *Española de Ciencia y Tecnología de Alimentos, 32*(1), 3-17.
776 Renard, C. M. G. C., & Ginies, C. (2009). Comparison of the cell wall composition for flesh
777 and skin from five different plums. *Food Chemistry, 114*(3), 1042-1049.
778 Ridley, B. L., O'Neill, M. A., & Mohnen, D. A. (2001). Pectins: Structure, biosynthesis, and
779 oligogalacturonide-related signaling. *Phytochemistry, 57*(6), 929-967.
780 Robertson, J. A., de Monredon, F. D., Dysseler, P., Guillon, F., Amado, R., & Thibault, J.-F.
781 (2000). Hydration properties of dietary fibre and resistant starch: A European
782 collaborative study. *LWT-Food Science and Technology, 33*(2), 72-79.
783 Saeman, J. F., Moore, W. E., Mitchell, R. L., & Millett, M. A. (1954). Techniques for the
784 determination of pulp constituents by quantitative paper chromatography. *Tappi,*
785 *37*(8), 336-343.
786 Saunders, M., Bunggyoo, K., Maes, C., Akle, S., & Zahr, M. (2012). Primal-Dual Interior
787 Method for Convex Objectives. http://web.stanford.edu/group/SOL/software/pdco/.
788 (Accessed 11 December 2020).
789 Sila, D. N., van Buggenhout, S., Duvetter, T., Fraeye, I., de Roeck, A., van Loey, A., &
790 Hendrickx, M. (2009). Pectins in processed fruits and vegetables: Part II - Structure-
791 function relationships. *Comprehensive Reviews in Food Science and Food Safety,*
792 *8*(2), 86-104.

793 Singh, N., Inouchi, N., & Nishinari, K. (2005). Morphological, structural, thermal, and
794 rheological characteristics of starches separated from apples of different cultivars.
795 *Journal of Agricultural and Food Chemistry, 53*(26), 10193-10199.
796 Szczesniak, A. S., & Kahn, E. L. (1971). Consumer awareness of and attitudes to food
797 texture- I: Adults. *Journal of Texture Studies, 2*(3), 280-295.
798 Thibault, J. F., Renard, C. M. G. C., Axelos, M. A. V., Roger, P., & Crepeau, M. J. (1993).
799 Studies of the length of homogalacturonic regions in pectins by acid hydrolysis.
800 *Carbohydrate Research, 238*, 271-286.
801 Tjan, S. B., Voragen, A. G. J., & Pilnik, W. (1974). Analysis of some partly and fully
802 esterified oligogalactopyranuronic acids by P.M.R. spectrometry at 220 MHz.
803 *Carbohydrate Research, 34*(1), 15-32.
804 Van Buren, J. P. (1979). The chemistry of texture in fruits and vegetables. *Journal of Texture*
805 *Studies, 10*(1), 1-23.
806 Waldron, K. W., Parker, M. L., & Smith, A. C. (2003). Plant cell walls and food quality.
807 *Comprehensive Reviews in Food Science and Food Safety, 2*(4), 101-119.
808 Waldron, K. W., Smith, A. C., Parr, A. J., Ng, A., & Parker, M. L. (1997). New approaches to
809 understanding and controlling cell separation in relation to fruit and vegetable texture.
810 *Trends in Food Science & Technology, 8*(7), 213-221.
811 Zykwinska, A. W., Ralet, M.-C., Garnier, C. D., & Thibault, J.-F. (2005). Evidence for in
812 vitro binding of pectin side chains to cellulose. *Plant Physiology, 139*(1), 397-407.

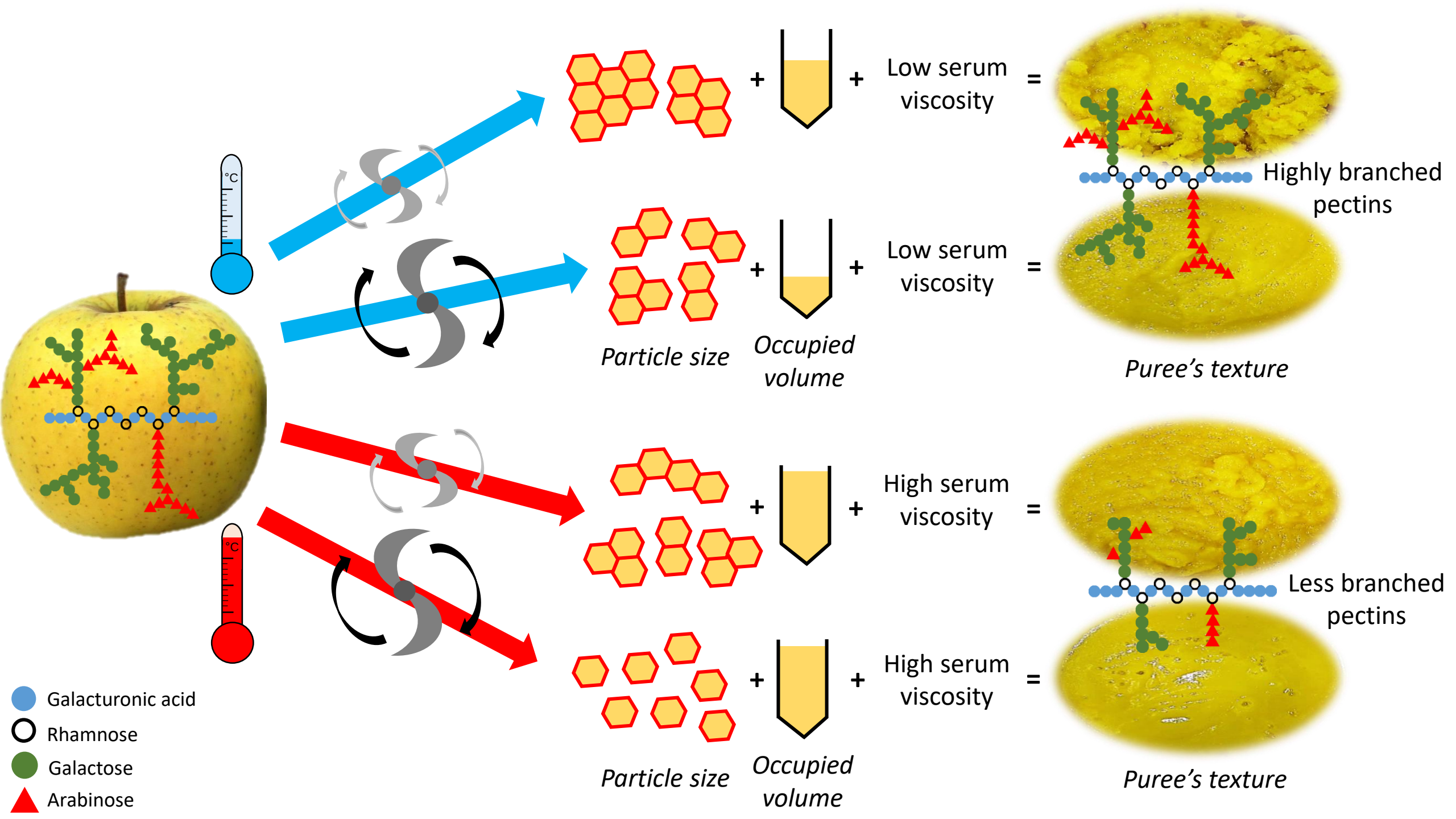
°C
°C
Low serum viscosity
Highly branched pectins
Particle size
Occupied volume
Low serum viscosity
Puree's texture
High serum viscosity
Less branched pectins
Particle size
Occupied volume
High serum viscosity
Puree's texture
Galacturonic acid
Rhamnose
Galactose
Arabinose